Investigation of Carbon Black/Ultra-High-Molecular-Weight-Polyethylene Nanocomposites Manufactured by Compression Molding and Equal Channel Angular Extrusion

KATERYNA MIROSHNICHENKO¹, TANISLAV BUKLOVSKYI¹, IGOR TSUKROV¹, REBECCA J. THOMSON², PEDER C. SOLBERG², AFTON K. LIMBERG² and DOUGLAS W. VAN CITTERS²

ABSTRACT

Conductive carbon black (CCB) reinforced ultra-high molecular weight polyethylene (UHMWPE) polymers are investigated by micro-computed tomography, scanning electron microscope, and mechanical testing. The composites are manufactured by two techniques: compression molding (CM) and equal channel angular extrusion (ECAE). It is observed that electrical conductivity increases for the composites with the higher concentration of CCB inclusions without significant loss of tensile toughness. At the same time, ECAE procedure decreases the observed thickness of the CCB-rich layer and decreases electrical conductivity of the UHMWPE composites as compared to CM. Concentration of carbon inclusions in CCB-rich layer was evaluated for different weight fractions of CCB in the overall composite. Preliminary studies indicate that ECAE doesn't change the orientation and elongation of UHMWPE particles in the CM consolidated composites.

COMPRESSION MOLDING AND EQUAL CHANNEL ANGULAR EXTRUSION OF UHMWPE WITH CONDUCTIVE CARBON BLACK

Ultra-high molecular weight polyethylene (UHMWPE) offers a list of exceptional properties, such as mechanical strength, ductility, biocompatibility, and wear resistance, which makes it the primary choice for the polymeric component in total joint replacement. The addition of carbon allotropes, e.g. carbon black powders, to UHMWPE offers potential benefits including added conductivity, increased wear resistance, and introduction of micro-tracers for understanding microstructural behavior and monitoring damage.

In this paper, we consider UHMWPE polymers with conductive carbon black (CCB) inclusions manufactured by compression molding (CM) and equal channel angular extrusion (ECAE). Compression molding is a common polymer manufacturing process for thermosets, thermoplastics, as well as elastomers and natural rubbers. It produces high-volume, dimensionally precise, high-strength, temperature resistant parts with good surface quality [1]. ECAE was initially

¹University of New Hampshire, Durham, NH 03824 USA ²Dartmouth College, Hanover, NH 03755 USA

proposed to change the microstructure of metals without changing the cross-section of a billet [2, 3], and was later applied to polymers and polymer-based composites [4-10].

For both CM and ECAE samples, the set up shown in Fig.1 was used. The dies are made of steel; the cross-section is a square $5 \text{ cm} \times 5 \text{ cm}$; the length of vertical and horizontal channels is 16.5 cm; the pressure plungers are made of aluminum.

First, UHMWPE powder was combined with CCB inclusions at a ratio of 1%, 1.5%, 2.5%, 5%, and 10%, and mechanically mixed for 25 minutes. Then, the mixture was loaded into the extrusion channel and compressed at 400 psi with a back pressure plunger. To produce the CM samples, the mixture was consolidated at 162.5 °C for 2.5 hours. To produce the ECAE samples, the consolidated samples were then extruded at a rate of 0.1 in/s, which correlates to a shear strain rate of 0.01%/s. After extrusion or compression molding, sample billets were allowed to cool at room temperature for 24 hours.

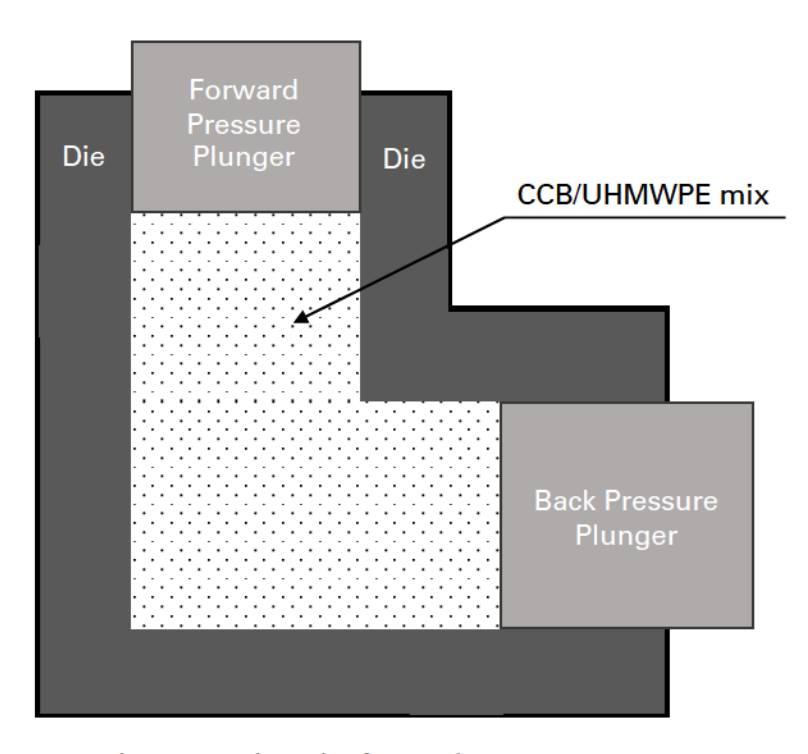


Figure 1. A schematic of CM and ECAE setup.

MEASUREMENTS OF THE EFFECTIVE CONDUCTIVITY AND TENSILE TOUGHNESS OF CCB/UHMWPE NANOCOMPOSITES

Two types of tests were conducted to characterize CCB/UHMWPE nanocomposites with different weight fractions of the CCB inclusions: electrical conductivity and tension. After microtoming 200 µm sections, the samples were produced following ASTM D638 with a Type V modified specimen to be suitable for both conductivity measurements and tensile testing. To measure conductivity, alligator clamps were placed 23 mm apart on tensile samples with only the blunted teeth attached to avoid creating stress concentrators. The alligator clamps were attached to a PalmSens3 potentiostat (Palmsens BV, Houten, The Netherlands) which applied a constant 5V potential. The measurements were conducted for 10 seconds at a frequency of 10 Hz. Each sample was tested twice to account for user error in placement of the alligator clamps on the samples. Conductivity allows for the measurement of whether conductive pathways exist within the composite materials and the subsequent resistivity.

The tensile testing was conducted on the same samples using an Instron 5540 (Norwood, MA) equipped with a 2 kN load cell and pneumatic grips. To measure the strain of the sample during testing, a video extensometer was employed. The testing was performed at an extension rate that allowed for a 100% strain per minute in the gauge region, which corresponded to a crosshead speed of approximately 25.4 mm/min. The BlueHill 2 software was used to record stress-strain curves, which were later analyzed using a customized MATLAB code to calculate tensile toughness, elongation at break, 0-slope yield, and ultimate tensile stress.

The results of the tests are presented in Fig. 2. At least 30 samples were tested for each weight fraction and fabrication method. It can be seen that electrical conductivity significantly increases with the increase of the weight fraction of CCB inclusions for both CM and ECAE processed nano-composites (Fig. 2a). This increase is achieved with only minimal reduction of tensile toughness (Fig. 2b). It is observed that ECAE process reduces electrical conductivity for composites with low weight fraction (1%, 1.5%, 2.5%), while increasing it for composites with 5 wt%. A possible explanation of this behavior will be discussed in the next section.

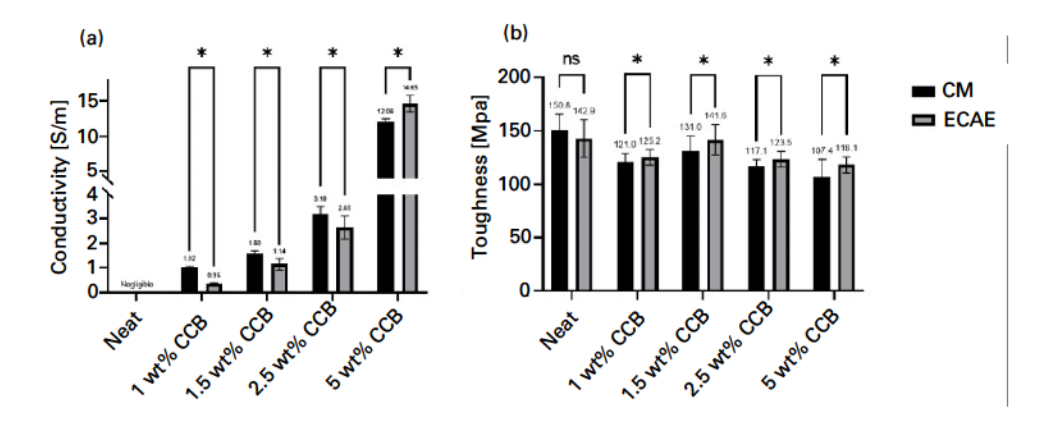


Figure 2. Dependence of (a) electrical conductivity and (b) tensile toughness of CCB/UHMWPE composites on weight fraction of CCB inclusions and fabrication method. Symbol * indicates statistical significance as tested by a linear contrast 2-way ANOVA.

X-RAY µCT STUDIES

To investigate the effects of CM and ECAE manufacturing processes on distribution of CCB in CCB/UHMWPE composites, micro-computed tomography (μ CT) imaging was conducted on 1 wt%, 2.5 wt%, 5 wt%, and 10 wt% of CCB samples. μ CT was performed on ZEISS Xradia 610 Versa microscope with the following settings: voltage – 60 kv, power – 6.5 W, obj – 0.4X, binning – 1, exposure – 1s, filter – air.

Fig. 3 shows examples of 3D views and 2D cross-sections of microstructures for 1 wt% and 5 wt% CCB/UHMWPE samples produced via CM and ECAE techniques. The scanned volume was $0.49 \times 0.5 \times 0.52$ mm. Gray color corresponds to UHMWPE particles. The volume fraction of white regions is higher than the total volume fraction of all CCB inclusions in the composite. This indicates that the white color corresponds to a high concentration mixture of CCB inclusions in UHMWPE matrix. This mixture is located mostly in the layers surrounding the UHMWPE particles. The estimates for the CCB-rich layers' thickness and concentration of CCB particles are provided in the following subsections.

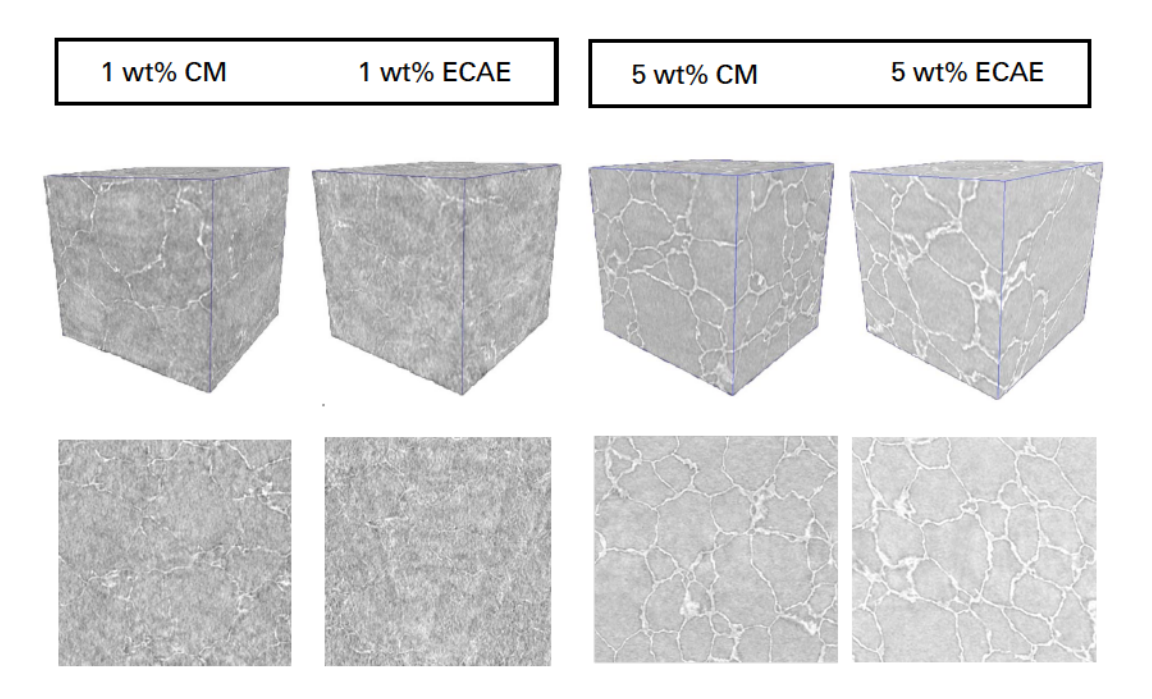


Figure 3. Examples of microstructures of CCB-reinforced samples.

Dependence of CCB-rich layer thickness on weight % of CCB inclusions and fabrication method

ORS Dragonfly (Object Research Systems, Canada) was used to extract the observed thickness of CCB-rich layer. Two approaches were considered. The first approach included direct measurement utilizing the Dragonfly digital ruler. First, four random images representing different cross-sectional areas of each sample were chosen from the CT-scans. Then, layer thicknesses were measured at 25 randomly selected locations for each sample. Finally, based on the gathered data, the average thickness of the layers was calculated. The results of the measurements are summarized in Fig. 4 and Table I. As can be seen from Fig. 4, the thickness of the layer increases with the increase of wt% and the thickness is consistently larger for CM samples when compared to ECAE.

The second approach was based on the 3D volume fraction of CCB-rich layer V_L extracted from the images. This data was processed assuming the layers are uniformly distributed around each UHMWPE particle of an idealized shape (either spherical or cubical), as seen in Fig. 5. Based on this assumption, the theoretical average layer thickness t was calculated from the equations presented in Figure 5 (both shapes produced the same value).

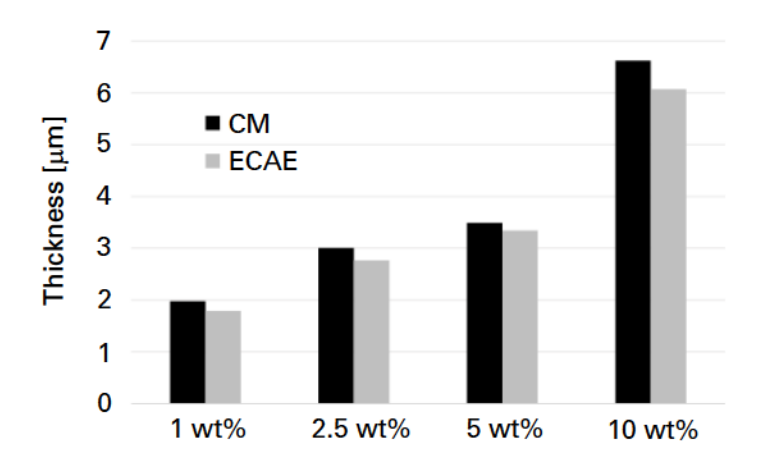


Figure 4. Comparison of the averaged thicknesses of CCB-rich layers in CM and ECAE manufactured samples.

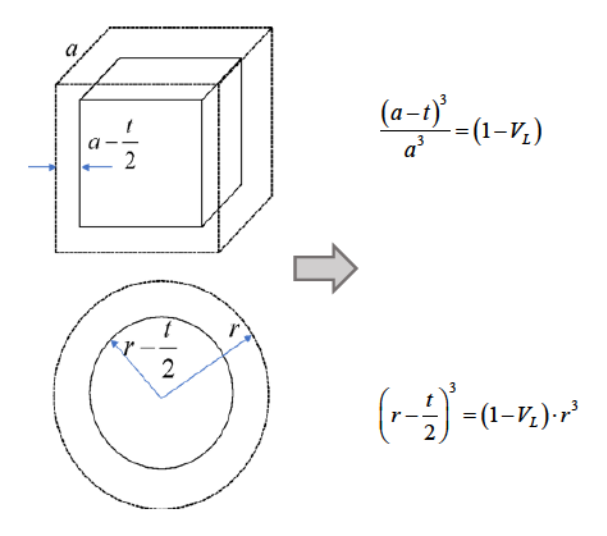


Figure 5. Schematics and equations used for calculation of CCB-rich layer thicknesses.

Comparison of the CCB-rich layer thickness measurements obtained by both approaches is given in Table I. It can be seen that both approaches indicate that ECAE reduces the observed thickness of the layer. A possible explanation is that shearing deformation during the extrusion process dissipates (diffuses) some individual CCB inclusions into the material, so they are no longer a part of high concentration regions and thus cannot be detected by μ CT. Note that direct 2D measurements provide higher values for the layer thickness because 2D cross-sections will not necessarily be normal to the layer, so not the shortest distance between the adjacent UHMWPE particles is measured.

TABLE I. EVALUATION OF CCB-RICH LAYER THICKNESS

Samples	Calculated from 3D [µm]			Measured in Dragonfly [μm]		
	CM	ECAE	% decrease in t	CM	ECAE	% decrease in t
1%wt	0.67	0.6	10.4	1.98	1.79	9.6
2.5%wt	1.25	1.08	13.6	3.01	2.76	8.3
5%wt	2.11	2.01	4.7	3.49	3.34	4.3
10%wt	4.32	4.21	2.5	6.62	6.07	8.3

We observe that ECAE reduces thickness of CCB-rich layer. This reduction, apparently, has a different effect on low weight fraction of CCB and high weight fraction of CCB composites. For low weight fraction composites, few conductive paths exist, and they are interrupted by ECAE reducing the overall electrical conductivity. For higher weight fraction composite (5% of CCB), there are more conductive pathways. In this case, ECAE smooths out some of the CCB clusters and helps with formation of new conductive pathways.

Evaluation of volume fraction of CCB in CCB-rich layers

White layers surrounding each UHMWPE particle in μ CT images (as shown in Fig. 3) contain high concentration of carbon inclusions, as schematically represented in Fig. 6. The volume fraction ($V_{c/L}$) of the inclusions in the layer can be evaluated as a ratio of the volume fraction of inclusions in the overall composite (V_{CCB}) and the volume fraction of white-colored regions in the μ CT images:

$$V_{c/L} = \frac{V_{CCB}}{V_L} \tag{1}$$

where

$$V_{CCB} = \frac{W_{CCB}}{W_{CCB} + (1 - W_{CCB}) \frac{\rho_c}{\rho_m}},$$
(2)

 W_{CCB} is the weight fraction of the inclusions in the composite, $\rho_c = 1.9$ g/cm³ [11] is the density of CCB inclusions, and $\rho_m = 0.93$ g/cm³ [12] is the density of UHMWPE. The results are summarized in Table II.

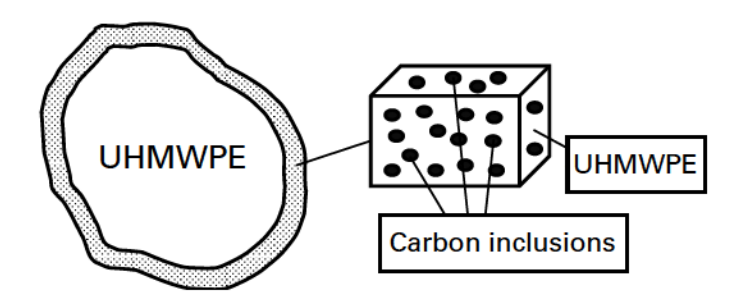


Figure 6. Schematics of UHMWPE particle surrounded by carbon-rich layer.

TABLE II. VOLUME FRACTIONS OF CCB-CONTAINING PHASE

Samples	V _{CCB}	V_L	V _{c/L}
0.5%wt	0.25	0.4	0.61
1%wt	0.49	1.5	0.33
1.5%wt	0.74	2.3	0.32
5%wt	2.5	5.5	0.46
10%wt	5.16	9.0	0.57

ORIENTATION AND SHAPE DISTRIBUTION OF UHMWPE PARTICLES

A preliminary numerical investigation was performed to determine whether the ECAE process changes the shape and orientational distributions of UHMWPE particles in CCB/UHMWPE nanocomposites. The investigation utilized scanning electron microscope (SEM) images produced with the Tescan SEM at 2kV. The 1 cm² samples were not gold coated to be able to observe the contrast between CCB-rich boundaries and UHMWPE particles. Two images were considered: 10 wt% CCB/UHMWPE processed by CM and ECAE, see Fig. 7.

Figure 8 presents the framework of image processing and analysis procedure. The image processing was performed utilizing Image J (Fiji) software. Initial pre-processing of .tiff files involved the merging of image channels followed by the Rudin-Osher-Fatemi Total Variation (ROF) denoising and Gaussian smoothing. The resultant grey-scale images were binarized to obtain high-quality black-and-white output. For binarization, the Image J MultiThreshold was utilized – the best image was selected out of 15 results produced by different local and global threshold algorithms.

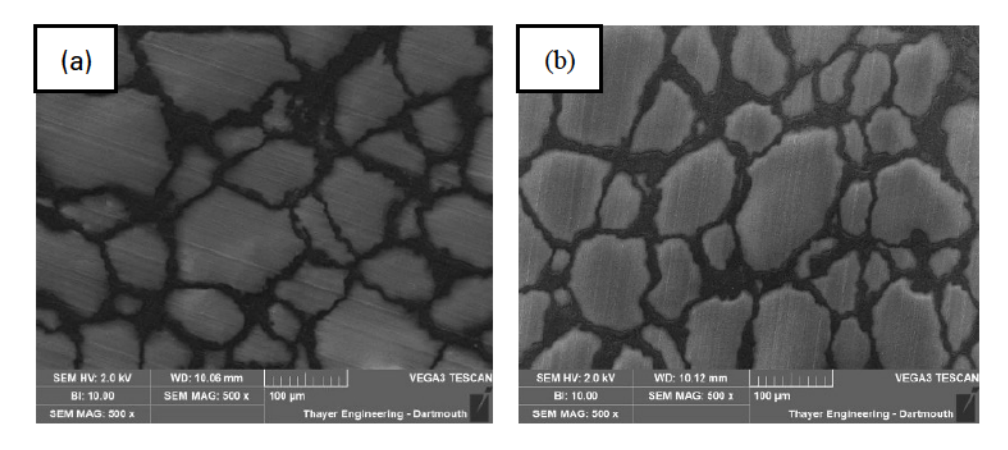


Figure 7. SEM images of the composite processed by (a) CM and (b) ECAE.

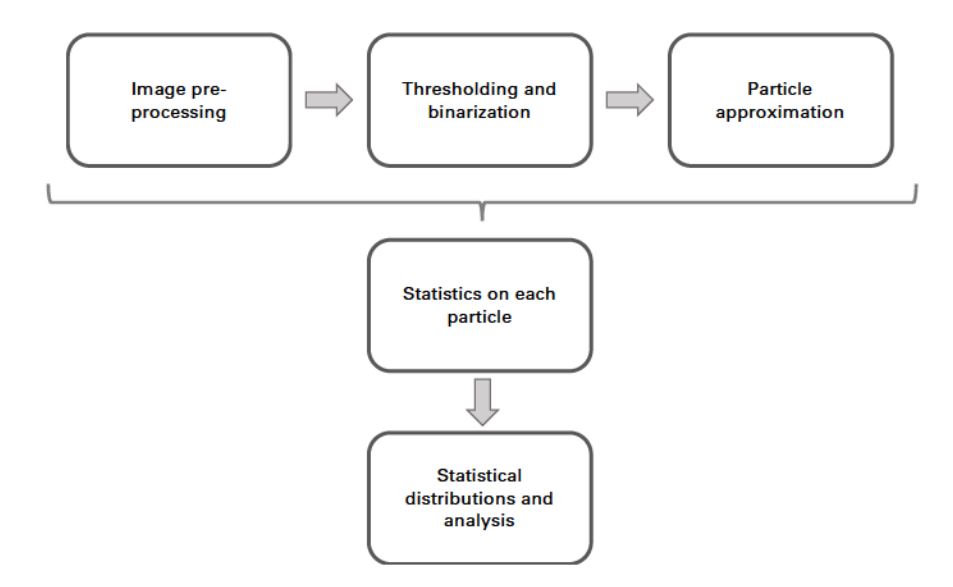


Figure 8. Orientation and shape analysis framework.

For statistical analysis of the microstructure, the UHMWPE particle shapes were approximated by ellipses. Application of the internal iterative procedure in Image J results in the distribution of equivalent elliptical shapes shown in the last column of Figure 9. Each ellipse is characterized by its major and minor axes a and b, and the orientation ϕ of the major axis a with respect to the global x-axis, see Figure 9.

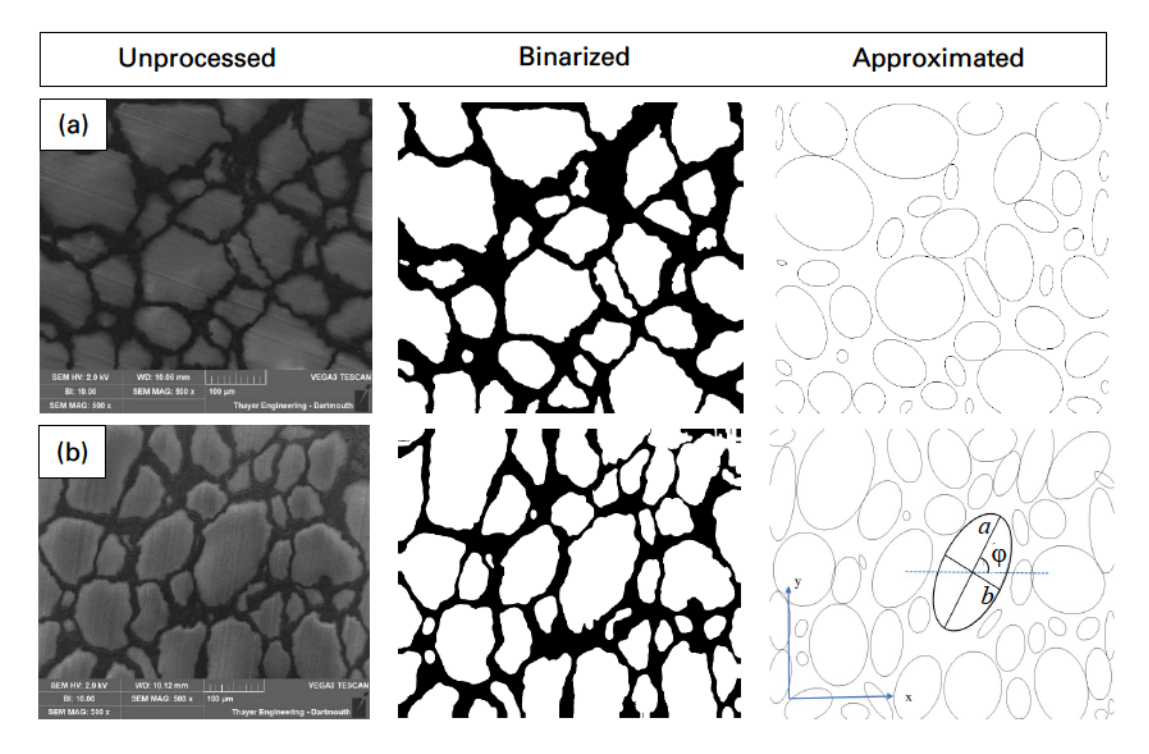


Figure 9. Approximation of UHMWPE particle shapes by ellipses for (a) CM and (b) ECAE processed composite.

There are two potential ways to describe elongations of the UHMWPE particle shapes based on their 2D images, circularity c and roundness r:

$$c = \frac{4\pi \cdot A}{L} \tag{3}$$

$$r = \frac{4 \cdot A}{\pi d^2} = \frac{b}{a} \text{ (for ellipse)}$$
 (4)

where A is the area of the particle, d is the axial maximum dimension, and L is the perimeter of the shape. Roundness was selected as a simple and robust shape metric (independent of local irregularities of the boundary). The comparison between CM and ECAE-manufactured composites is given in Fig. 10 and Fig. 11. Fig. 10 provides statistical distributions of orientations; Fig. 11 provides statistical distributions of roundness. Two sets of data are presented. The first set provides information on the orientation and shape distributions without taking into account the size of particles (the smaller and larger particles are included with the same weight). In the second set, the contributions of particles are taken with the weight proportional to their area. In all figures, the normal Gaussian distribution based on the mean and standard deviation values is also provided.

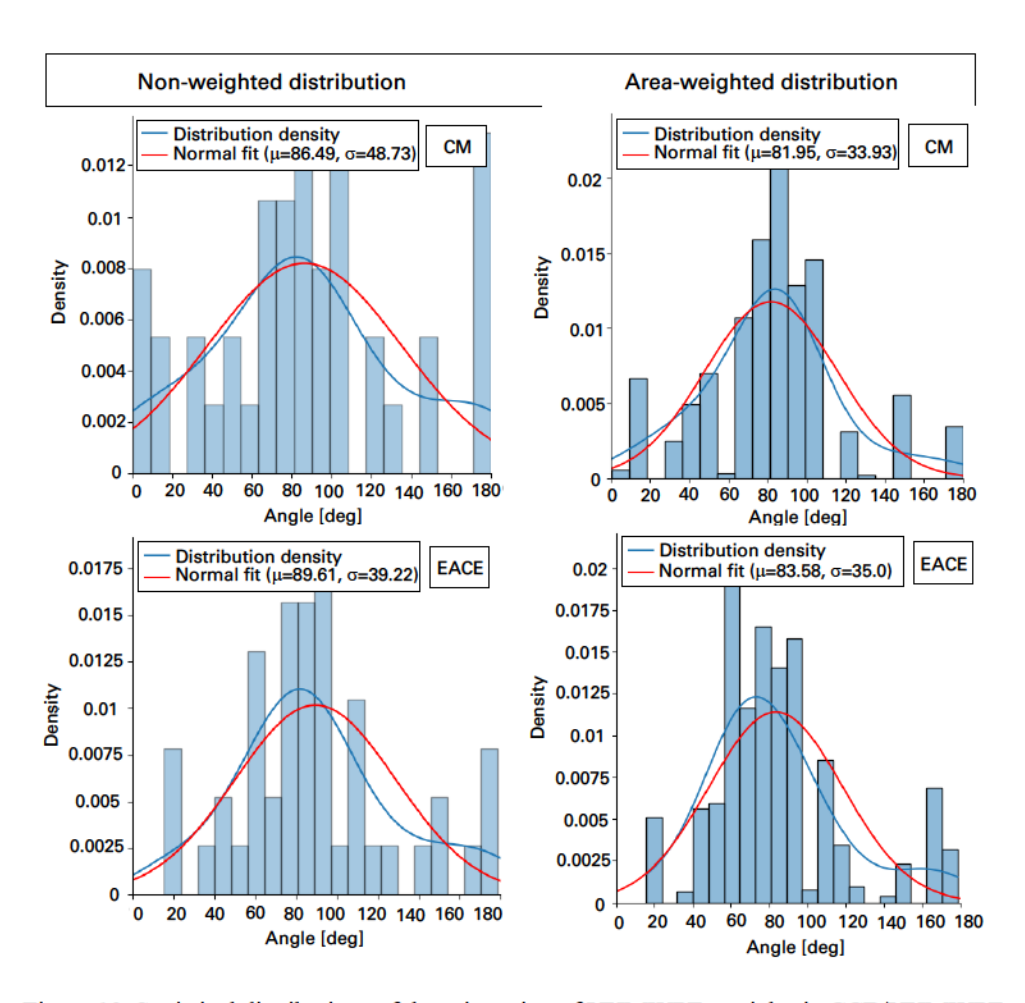


Figure 10. Statistical distributions of the orientation of UHMWPE particles in CCB/UHMWPE composites manufactured by CM and ECAE.

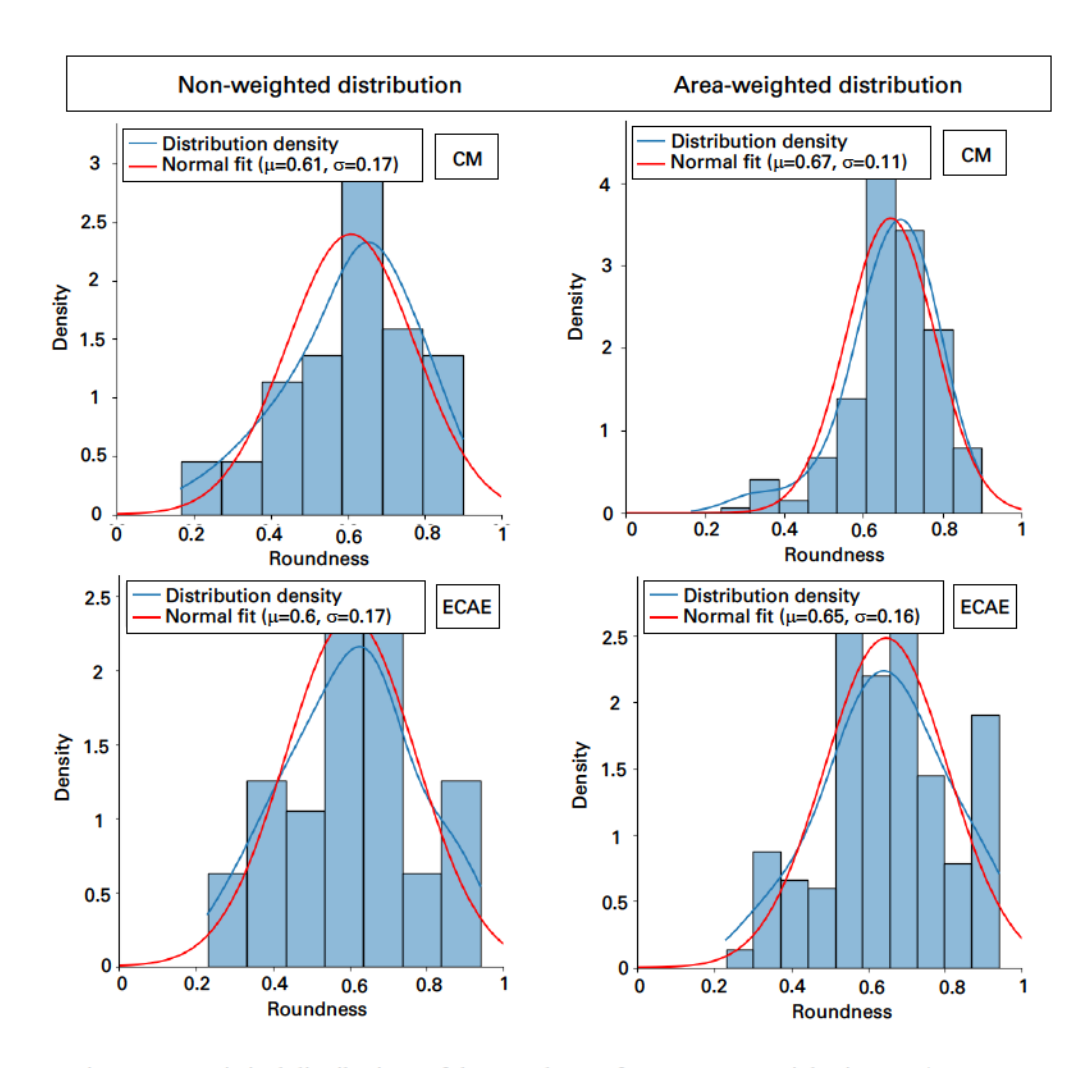


Figure 11. Statistical distributions of the roundness of UHMWPE particles in CCB/UHMWPE composites manufactured by CM and ECAE.

The results of the preliminary study, summarized in Fig. 10 and Fig. 11, indicate that the ECAE procedure does not significantly change the elongation and orientation distributions of UHMWPE particles in CCB/UHMWPE composites. However, it has to be noted that this study was conducted on two 2D images only. To produce conclusive results, a much larger set of images should be processed with the 3D nature of particles taken into account.

CONCLUSIONS

Addition of conductive carbon nanoparticles to UHMWPE changes mechanical and conductive properties of the polymer and provides opportunities to introduce electric sensors for understanding microstructural behavior and monitor damage.

Two manufacturing processes, compression molding and equal channel angular extrusion, were considered in this paper. Analysis of μ CT images shows that for both processes, it is possible to achieve almost uniform distribution of carbon inclusions

around UHMWPE particles. However, the thickness of CCB-rich layer is lower for ECAE-manufactured materials, mostly due to the smoothing of CCB clusters.

Testing reveals that the electrical conductivity of the composites increases with higher concentrations of CCB inclusions, while the tensile toughness remains largely unaffected. Moreover, it is observed that the ECAE procedure leads to a decrease in the electrical conductivity of the UHMWPE composites due to the reduction of the conductive layer.

To facilitate the numerical modeling of the composites, the concentration of carbon inclusions within the CCB-rich layers is evaluated for various weight fractions of CCB within the overall composite structure.

Preliminary findings suggest that orientation and elongation of UHMWPE particles in the CM consolidated composites remain unaffected by the ECAE procedure. Though, it is important to note, that study was limited to analyzing two 2D images only. In order to obtain definitive conclusions, a significantly larger set of images should be examined, considering the three-dimensional nature of the particles.

ACKNOWLEGEMENTS

The authors acknowledge funding by the National Science Foundation EPSCoR award (#1757371).

REFERENCES

- Park, C.H., Lee, W.I. 2012. "Compression Molding in polymer matrix composites" in Manufacturing Techniques for Polymer Matrix Composites (PMCs), S.G Advani, and K-T. Hsiao, eds. Woodhead Publishing, pp. 47-94.
- Segal, V. 1999. "Equal channel angular extrusion: from macromechanics to structure formation," Mater. Sci. Eng., A 271: 322–333.
- 3. Segal, V. 2004. "Engineering and commercialization of equal channel angular extrusion (ECAE)," *Mater. Sci. Eng.*, A 386: 269–276.
- 4. Beloshenko, V., Y. V. Voznyak, I. Y. Reshidova, M. Naït-Abdelaziz, and F. Zairi. 2013. "Equal-Channel Angular Extrusion of Polymers," *J. Polym. Res.*, 20(12): 1–13, 322.
- Sue, H., H. Dilan, and C. K. Y. Li. 1999. "Simple Shear Plastic Deformation Behavior of Polycarbonate Plate Due to the Equal Channel Angular Extrusion Process. I: Finite Element Methods Modeling," *Polym. Eng. Sci.*, 39(12): 2505–2515.
- Cook, D., H. H. Chun, and D. W. Van Citters. 2019. "Mechanical and electrical characterization of two carbon/ultra high molecular weight polyethylene composites created via equal channel angular processing," J. of Eng. Mater. Technol., 141: 1-7.
- Reinitz, S., A. J. Engler, E. M. Carlson, and D. W. Van Citters. 2016. "Equal channel angular extrusion of ultra-high molecular weight polyethylene," *Mater. Sci. Eng. C.*, 67: 623–628.
- Favreau, H., K. Miroshnichenko, P. C. Solberg, I. Tsukrov, and D. W. Van Citters. 2022. "Shear enhancement of mechanical and microstructural properties of synthetic graphite and ultra-high molecular weight polyethylene carbon composites," *Journal of Applied Polymer Science*, 139 (20).
- Vasylevskyi, K., I. Tsukrov, K. Miroshnichenko, S. Buklovskyi, H.J. Grover, and D. W. Van Citters. 2021. "Finite Element Model of Equal Channel Angular Extrusion of Ultra High Molecular Weight Polyethylene," *Journal of Manufacturing Science and Engineering*, 143 (12).
- Miroshnichenko, K., S. Buklovskyi, K. Vasylevskyi, I. Tsukrov, H. J. Favreau, R. J. Thomson, P. C. Solberg, and D. W. Van Citters. 2022. "Characterization and Modeling of Carbon Black/Ultra-High-Molecular-Weight-Polyethylene Nanocomposites Manufactured with Equal

- Channel Angular Extrusion," Proceedings of 20th International Conference on Fracture and Damage Mechanics, Malaga, Spain, 5-7 September.
- Wypych, G. 2014. "3.2.1 Carbon black" in *Databook of Antistatics*, Elsevier, pp. 245-271.
 Hunt, B.J. and T.J. Joyce. 2016. "A Tribological Assessment of Ultra High Molecular Weight Polyethylene Types GUR 1020 and GUR 1050 for Orthopedic Applications," Lubricants, 4(3), 25.